Annu. Rev. Biomed. Eng. 2004. 6:427–52
doi: 10.1146/annurev.bioeng.6.040803.140100

First published online as a Review in Advance on April 13, 2004

FRACTAL ANALYSIS OF THE VASCULAR TREE IN THE HUMAN RETINA

Barry R. Masters
Formerly, Gast Professor, Department of Ophthalmology, University of Bern, 3010 Bern, Switzerland; email: brmail2001@yahoo.com

Key Words fractals, fractal structures, eye, bronchial tree, retinal circulation, retinal blood vessel patterns, Murray Principle, optimal vascular tree, human lung, human bronchial tree

■ **Abstract** The retinal circulation of the normal human retinal vasculature is statistically self-similar and fractal. Studies from several groups present strong evidence that the fractal dimension of the blood vessels in the normal human retina is approximately 1.7. This is the same fractal dimension that is found for a diffusion-limited growth process, and it may have implications for the embryological development of the retinal vascular system. The methods of determining the fractal dimension for branching trees are reviewed together with proposed models for the optimal formation (Murray Principle) of the branching vascular tree in the human retina and the branching pattern of the human bronchial tree. The limitations of fractal analysis of branching biological structures are evaluated. Understanding the design principles of branching vascular systems and the human bronchial tree may find applications in tissue and organ engineering, i.e., bioartificial organs for both liver and kidney.

CONTENTS

INTRODUCTION

Scope of the Review

This review presents a critical evaluation of the literature on the application of fractal measurements to the retinal circulation of the living normal human retina. The goals of this research are to determine the fractal dimension of the retinal vascular branching patterns and to infer the mechanism and optimization principles of its formation. Where it is appropriate, a discussion of the optimization principles consistent with the branching structure of the human bronchial tree and other organs is included.

The vascular system in the human retina has a unique property: It is easily observed in its natural living state in the human retina by the use of a retinal camera (1). The retinal circulation is an area of active research by numerous groups, and there is general experimental agreement on the analysis of the patterns of the retinal blood vessels in the normal human retina. However, studies of the vascular systems in the human lung and the human heart are made from resin corrosion casts because the patterns of the vessels in these organs are not directly observable in the living person. For these reasons, I have restricted the main portion of this review to the retinal circulation in the normal living human retina.

This review covers the following topics: the historical development of fractal analysis, the various methods to determine the fractal dimension of branching vascular trees, fractal growth processes, the experimental results on the fractal analysis of the normal human retinal circulation, the implications of this pattern for both vasculariogenesis and diagnostics, the limitations of the experimental analysis and interpretation of the results, and, finally, a discussion of the optimal organization of vascular trees and the human bronchial tree.

This review covers studies of large vessels, arteries, and veins that are observed with a red-free fundus camera in the normal human eye. It is important to note that the major vessels feed and drain the small capillaries, which are the sites of exchange between the components of the blood (gas exchange, nutrient exchange) and the surrounding tissue.

The Role of Fractal Analysis in Biology and Medicine

A number of books serve as a good introduction to the topics of shape, pattern formation, scaling, and fractals in biology and medicine (2–6). The applications of fractal analysis in biology and medicine can be divided into two groups: (*a*) spatial analysis of shapes and branching patterns and (*b*) temporal analysis of time-varying signals. The applications of fractals to biology and medicine cover a wide range

of scale: molecules, cells, tissues, and organs (7). The goal of this methodology, as applied to branching structures in tissues and organs, is to determine the fractal dimension of these objects and structures and then to use this number as a classifier to discriminate the class of normal structures from abnormal and pathological structures.

During the early application of fractal geometry to medical diagnostics, preliminary studies attempted to demonstrate the diagnostic value of fractals in the diagnosis of retinal disease (36, 37, 70, 72, 74). For a diagnostic method to have clinical efficacy it should provide an early discriminant from the normal condition (including biological variability) and show appropriate sensitivity and specificity. Fractal analysis has utility in the ability to characterize the shapes of cellular organelles, cells, tissues, and organs. These shape descriptors may be shown to have sufficient sensitivity and specificity in diagnostic tests to discriminate the pathological from the normal. This has not been the case for the early diagnostics of retinal pathology based on fractal analysis of the blood vessel patterns in the retinal circulation. In the presence of severe retinal disease there are alterations in the patterns of the blood vessels; however, these vascular changes are easily observed with a retinal camera. For example, fractal geometry can be used to quantify the progression of severe proliferative diabetic retinopathy (70). But these severe alterations from the normal vascular patterns are readily observed with a retinal camera, and therefore this technique is not an important diagnostic method.

Most retinal microvascular abnormalities occur early in the disease process and are located in the capillaries and result in alterations of permeability (59, 80). These early vascular alterations are not detected by fractal analysis. The fractal analysis of the blood vessels in the retinal circulation is a global measure of the pattern of the blood vessels; as such, it is not sensitive to small alterations of a small region of the total pattern.

Alternatively, the fractal dimension can be used as an index of growth or development. An example of this type of fractal classification is the fractal analysis of neurons in which different classes of neurons are associated with a different fractal dimension (8–11). In addition, during the growth and development of neurons, the measured fractal dimension changes in a systemic way, and thus it provides a mathematical characterization of the development of the neuron associated with its increased branching during growth and development (12).

Fractal analysis has also been applied to branching structures in the heart (5, 13). These studies have shown that a number of cardiopulmonary structures are fractal in their design. Examples of such self-similar structures are the arterial and venous branching trees, the branching of some cardiac muscle bundles, the branching of the bronchial tree, and the branching of the His-Purkinje network.

Fractal geometry has also been used for the description of texture in medical images (14). Texture can be defined as the spatial distribution of intensity values in an image. For example, fractal methodology has been used for the classification of benign and malignant tumors from chest radiographs (15). The power spectrum of regions in chest radiographs has been subjected to fractal analysis to differentiate

between normal and nodular regions (16). Because the branching structure of the airways and the vessels of the lung show geometric self-similarity they can be modeled as a fractal (17, 18). An example of a diagnostic application is a study in which the fractal dimension has been used to discriminate normal lung from interstitial lung in computerized tomography (CT) images (18).

Another class of applications involves the study of branching biological structures and patterns. The bronchial tree and its branching design is the subject of several works (19–23).

An important topic for the application of fractal analysis is the branching trees of the vascular system in various tissues and organs. The following examples illustrate the diversity of biological branching vascular trees that have been analyzed as fractals: the morphometry of the small pulmonary arteries in man (24), the branching vascular system in the kidney (25), the branching vascular system in the heart (13), and the retinal circulation in the human retina (26–28). The goal of these studies is to determine the fractal dimension that characterizes the vascular systems of these organs. From a determination of the fractal dimension, inferences can be made on the mechanisms of their pattern formation. The fractal dimension may also provide evidence for a particular fractal growth process and its physiological correlates. For example, Tsonis & Tsonis (29) studied the fractal property of blood vessels in the developing embryo and proposed a diffusion-limited aggregation model.

A second class of fractal studies in physiology and medicine involves the temporal domain; for example, the one-dimensional time series of physiological signals and processes (30). Fractal signals are signals that have detail on all temporal scales; they are statistically self-similar. Applications of fractals in the time domain include the following: the analysis of normal and pathological brain activity from electroencephalogram data, studies of normal and abnormal cardiac electrical activity (31), and the application of fractals to ion channel kinetics (32).

How is Fractal Analysis Useful to Study Vascular Systems?

Physiologists have studied the vascular system for many years. These studies cover the spatial scales from angiogenic molecules to the global pattern of the vascular systems. For example, at the molecular level, there are active investigations on the molecular signals and mechanisms of blood vessel formation and development and studies on compounds that can block angiogenesis in tumors (33–35). At the global level, investigations of corrosion casts of vascular systems within the heart, lungs, and kidneys aim to characterize the branching patterns of blood vessels within these organs (25).

Scientists who study the patterns of the vascular system may pose the following questions: How can we characterize the pattern of the blood vessels? What parameters need to be measured? And finally, is there a theoretical model or optimization principle that is consistent with both the pattern and the computer simulations that yield the observed pattern of blood vessels?

Typically, what is measured in a vascular system are the spatial properties and the blood flow velocities within subsets of the vascular system (24). Experimentally, this is a geometrical determination of the blood vessel diameters, lengths, and branching angles, together with physiological blood flow measurements. These parameters are determined on a scale from the major artery that provides the input down to the capillary bed and to the veins that drain the tissue. The measured parameters are then examined to determine goodness of fit with theoretical optimization models of blood flow, bifurcation angles, and branching lengths.

A new and different approach to the study of vascular systems is to use fractal analysis to characterize the blood vessel patterns in the normal human retinal circulation (36). The first step is to determine if the vascular pattern can be characterized as a fractal (methods and concepts are developed in subsequent sections) and then to measure the fractal dimension, which is a number that characterizes the distribution of the branching vascular system in two-dimensional space. Finally, it would be both interesting and useful to determine if the growth processes that are consistent with the fractal dimension of the vascular system can be derived from one or more of the global optimization principles for blood vessel branching systems. An understanding of the design principles of the human vascular system may have applications in the synthetic design of vascular systems in tissue and organ engineering, i.e., bioartificial organs for both liver and kidney.

This review is limited to the development of the normal retinal circulation; however, there is another aspect of the development of the vascular system following injury: neovascularization. A fractal model was used to simulate patterns of corneal neovascularization by inverted diffusion-limited aggregation (37).

HISTORICAL DEVELOPMENT OF FRACTAL ANALYSIS

Anyone who marvels at a tree, a leaf, a river system, or a lightning bolt must wonder about these branching patterns and their formation. The underlying unity of patterns in nature can be mathematically analyzed in terms of their scaling relations. This methodology is a sequel to the work of D'Arcy Thompson on scaling relations and biological structure and function during the early 1900s (38).

Throughout history, thinkers have wondered about the relations between numbers and physical reality (39, 40). First, someone discovered a relationship between objects (biological and nonbiological) and numbers. Then, philosophers, mathematicians, and theologians offered their explanations. These activities, which began thousands of years ago, continue to occur in our time.

The Greeks were aware of the principle of similitude or scaling (41, 42). They developed a linear scaling relation they called the "golden section" or "golden mean." This scaling relation was used in Greek sculpture and architecture. Later, during the thirteenth century at Pisa, the golden mean was developed in terms of a

sequence of numbers that were later termed Fibonacci numbers (43). How did this happen? In 1201, a man named Leonardo of Pisa, whose nickname was Fibonacci, discovered the sequence while he was breeding rabbits. Four centuries later, Kepler determined the recursion formula for the Fibonacci series. The golden mean was renamed by Kepler, who chose the term "divine proportion." The sequence can be generated by starting with the number 1 and each additional term in the sequence is composed of the sum of the two preceding terms. For example: 1, 1, 2, 3, 5, 8, 13, ... The ratio of each number to its immediate predecessor approached the golden mean as a limit ($\sim$1.618...). The Fibonacci sequence appears in such diverse applications as biological scaling relations and the keys of a piano.

Natural structures seem to have a similar appearance when viewed at different magnifications. When the basic pattern is magnified, one can observe repeating levels of detail; thus, each level looks like the whole. Rivers, coastlines, and mountains are familiar examples. Biological patterns can also obey scaling relations; however, these examples may be less familiar. For example, trees are self-similar objects. As the magnification is changed, each smaller portion looks like the entire tree. This example illustrates the concept of self-similar. A self-similar object has structure on all length scales and every part is the same as the whole. There are also examples of self-similar objects in art, notably the paintings "The Great Wave" by K. Hokusai and "The Deluge" by Leonardo Da Vinci.

It is important to distinguish between the terms similar and self-similar. A photograph of a face and its enlargement have the same shape and are called similar. However, a small portion of the photograph, e.g., the mouth, when magnified does not look like the original face in the photograph. The idea of similarity also exists in geometry. Two polygons are similar if there are areas of correspondence between the vertices such that the corresponding sides of the polygons are proportional and the corresponding angles are equal. Self-similar objects have similar shapes over a range of scales. As explained by Mandelbrot (45), self-similar objects are formed from subregions that resemble the shape of the whole object.

There is a 2500-year linkage from the Greek geometer Pythagoras, to Euclid, to D'Arcy Thompson, to Mandelbrot. Throughout this period, there was a strong unity between geometry, art, and nature. The developments of fractal geometry by Mandelbrot and others over the past 30 years illustrates the generality of patterns and demonstrates the myriad connections between geometry, art, and natural forms and patterns (44, 45).

It was Mandelbrot who pioneered the applications of fractal concepts to describe complex natural shapes, forms, and patterns (45). In 1961, Richardson published a work in which he described a scaling relation for the length of coastlines. This related the measured length to the size of the length scale used, which was raised to an exponent of 1-D. Richardson did not assign any special significance to the quantity D, which was not an integer. It was Mandelbrot who interpreted D as a dimension, even though it was not an integer, and named it the fractal dimension (44, 45). He was able to generalize the idea and introduced the concept of fractal geometry. Mandelbrot coined the word fractal from the Latin fractus to describe

highly irregular patterns, shapes, and mathematical sets. The name comes from the fact that complex shapes can be described by a number, the fractal dimension, which is usually a fraction. This theory differs from our everyday concept of objects in Euclidean space, which have integer dimensions. In Euclidean space, a line has a dimension of 1, a planar object has a dimension of 2, and a volume has a dimension of 3. Fractal geometry is used to describe complex shapes, such as clouds or mountains, for which the fractal dimension can be a fraction between 2 and 3. These concepts are contained in the following quotation from Mandelbrot: "Clouds are not spheres, mountains are not cones, coastlines are not circles, and bark is not smooth, nor does lightning travel in a straight line (45)." It is the almost universal applicability of fractal concepts in describing objects from trees to coastlines to galaxies that demonstrates the elegance and power of these mathematical concepts. This review applies these fractal concepts to the branching pattern of the normal human retinal circulation and explores the implications for the mechanism of its development (46, 47).

What are Fractals?

Before one can apply fractal analysis to biological objects it is necessary to understand the definition of a fractal (4, 48). In the previous sections, the concept of self-similarity was illustrated and defined. Fractals or fractal objects are self-similar structures or scale-invariant structures (45). Fractals are objects that show self-similarity at different magnifications. The fractal dimension is a measure of the roughness of a fractal structure. It can be understood as a form of symmetry. Round objects, such as circles or disks, are symmetric under the operation of rotation. Fractals are symmetric under changes of scale, which means that fractals are invariant under a change of length scale. In other words, fractals look the same under various degrees of magnification or scale. This definition is true for regular or deterministic fractals, such as those that may be generated on a computer by joining together similar shapes according to an algorithm.

The fractals that are found in nature are called random fractals, and their structure shows self-similarity only in a statistical sense. Random fractals are better described by the term invariance rather than self-similarity. Fractals found in nature show scale invariance only over a finite range of scale (usually between two and four decades): from their smallest to their largest dimension. Another important property found in all fractals is that their density decreases with the distance from any fixed point on them.

In addition to regular and random fractals, there are also self-affine, or anisotropic, fractals (49, 50). Examples of self-affine fractals are fractal surfaces. The self-similarity of the regular fractals, or the statistical self-similarity of the random fractals, is equivalent to an isotropic rescaling of the dimension of length. The geometric properties remain the same in this case. However, in self-affine fractals, the scale invariance holds only if the lengths are rescaled differently along specific directions. Examples of self-affine fractals include single-valued, nondifferentiable

functions and the plot of the distance from the origin versus time for a particle undergoing one-dimensional Brownian motion. Another example of a self-affine fractal is the silhouette of a mountain range. For this type of image, the variation of the horizontal and the vertical coordinate scale differently. This behavior is very different from the self-similar boundary of a coastline in which the pattern scales the same in all directions.

An interesting class of fractals is called Laplacian fractals (51). The Laplace equation is the mathematical basis of their formation. The two components in the generation of a Laplacian fractal are the Laplace equation and randomness. Laplacian fractals are useful for modeling such diverse growth phenomena as snowflakes, lightning, and crystal growth and aggregation. The many diverse phenomena that form Laplacian fractals involve the Laplace equation with different physical fields. In dielectric breakdown, the field is the electrostatic potential. In the process of viscous fingering, the physical field is the pressure field, and in dendritic solidification, the diffusion of heat is involved (52).

How do fractal objects differ from ordinary Euclidean objects? For Euclidean objects the mass of the object (M) scales with a length raised to an integral power; for example, the power of three for a sphere, the power of two for a plane, and the power of one for a line. The mass of a solid sphere M(r) is proportional to the radius, r, of the sphere raised to the third power. Fractal objects also obey the mass-length scaling relation; however, the exponent (the fractal dimension, D) is not equal to the Euclidean dimension d. The exponent is, in general, nonintegral and less than the Euclidean dimension.

There are many patterns in nature that show ramified, open branching structures. These objects can be described by fractal geometry in the following manner. The random, scale-invariant objects have a volume V(r) or unit mass density, M, that is a function of the linear size or the radius, r, of the object. It is found empirically that

$$M(r) \approx r^{+D}, \tag{1}$$

where D equals the fractal dimension. Equation 1 applies to fractals when they are self-similar. In general, the fractal dimension $D < d$, where d equals the Euclidean dimension of the space in which the fractal is embedded. The value of D is usually a noninteger. For objects in the real world, there is an upper and a lower cutoff size for which the relation holds. The reader may wish to consult some of the books that are devoted to the mathematical analysis of fractals (48, 50).

BASIC PRINCIPLES OF FRACTAL ANALYSIS

Techniques to Determine the Fractal Dimension

The first step in the fractal analysis of an object or pattern is to determine its fractal dimension. There are several methods to determine the fractal dimension D of

an object over several bounded length scales (49, 53). Real objects are typically defined as fractal if a scaling relation can be demonstrated over several decades of scale: the upper bound being the size of the object and the lower bound being dependent on the resolution of the technique. The methods to determine the fractal dimension of random fractals include (*a*) box counting, (*b*) the mass-radius relation, and (*c*) the two-point density-density or pair correlation function method.

The computer method to determine the box-counting dimension is outlined below (44, 45, 54). The binary image is covered with square boxes of side length (L). The number of boxes (N) of side length L are counted and denoted as N(L). The size of the box is then incremented and the process is repeated. N(L) is tabulated versus the size of the box (L). A log-log plot of N(L) versus (L) is plotted, and a linear least squares regression is made to determine the slope of the plot. The slope of the linear region of the plot is −D, where D is the box-counting dimension that corresponds to the fractal dimension.

A second method, which is based on the same concept, involves the mass radius relation (44). A set of concentric circles with increasing radii are drawn centered on the point of the object. The mass (M) at a given radius (r), M(r), is determined as a function of the size of the radius. A log-log plot of M(r) versus r is plotted, and the slope gives the fractal dimension D.

A third method useful for random fractals is based on the scaling relation of the two-point density-density correlation function (55). The definition of the normalized density-density, or two-point correlation function, is shown in Equation 2,

$$\mathrm{C(r)} = 1/\mathrm{N} \sum_{\mathrm{r}'} \rho(\mathrm{r} + \mathrm{r}')\rho(\mathrm{r}'). \tag{2}$$

Another interpretation of C(r) is the normalized autocorrelation function. This equation gives the expectation value or probability of finding a particle at the position $\mathrm{r} + \mathrm{r}'$, if there is a particle at position r. N is the number of particles in the cluster. In Equation 2, ρ(r) equals the local density, i.e., $\mathrm{p(r)} = 1$ if the point belongs to the object; otherwise, it is zero. Usually, fractal objects are isotropic, which is equivalent to stating that the correlations are independent of direction; therefore, r is a scalar quantity. If the object is scale-invariant (the definition of a fractal), the correlation function is unchanged up to a constant by rescaling by an arbitrary factor f. This relation is shown in Equation 3,

$$\mathrm{C(fr)} = \mathrm{f}^{-\alpha}\mathrm{C(r)}, \tag{3}$$

where α is a noninteger greater than zero and less than d, the Euclidean dimension. This equation is satisfied by a power law decay of the local density in the fractal shown in Equation 4,

$$\mathrm{C(r)} = \mathrm{r}^{-\alpha}, \tag{4}$$

where the exponent α is equal to the embedding dimension minus the fractal dimension.

$$\alpha = \mathrm{d} - \mathrm{D} \tag{5}$$

The power law dependence shown in Equation 4 corresponds to the algebraic decay of the local density, as the density-density correlation function is proportional to the density distribution surrounding a given point. Because for real biological branching systems the density-density correlation function method requires the subjective determination of the straight portion of a curving function plot there is some error in the evaluation of the fraction dimension.

For real fractals, a plot of C(r) shows three regions. For small r, C(r) is small and rapidly increases. In the middle region, the cluster is scale-invariant, and C(r) decays with the slope of α. However, as r approaches the size of the object, the correlations rapidly approach zero.

The mass-radius technique probes the mass within a given length scale, whereas the density-density correlation function is an average over the entire cluster. Therefore, in small-scale simulations or in random patterns with a limited range of length scales, these two methods give slightly different values for the fractal dimension D.

Different analytical methods used to determine the scaling properties of real objects yield different measures of the fractal dimension. If the objects are isotropic, self-similar, and continuous, then the different methods should yield the same fractal dimension. There are a number of other computerized methods to determine the fractal dimension that are of special interest (53).

In some experimental studies, it is the projection of the object, rather than the object, that is studied. For example, the fractal analysis of the retinal circulation of the normal human retina is based on two-dimensional retinal images taken with a fundus camera. The retinal circulation is on a curved surface of the eye, and it is the projection of this image onto the image plane that forms the acquired photograph. One could ask the question, is the fractal dimension of the projection of an object equivalent to the fractal dimension of the object? The answer is yes. The projection of a fractal embedded in three dimensions to a plane does not change D as long a $D < d$. (56). They are equivalent as long as the measured fractal dimension D is less than the dimension of the space d in which the object is embedded. For the normal human retinal circulation, this is the case as the fractal dimension is 1.7 and the dimension of the two-dimensional space is 2.

Fractal Growth Processes

There are many growing, branching patterns that can be described by fractal geometry (39). These patterns are self-similar in a statistical manner. Another way of formulating this concept is that the volume of the object V(R) scales with the increasing size of R.

$$V(R) \sim R^{+D} \tag{6}$$

The fractal dimension D is usually a noninteger number, and $D < d$, where d is the Euclidean dimension of the space in which the fractal object is embedded.

There are several computer models to simulate fractal growth (52). However, only one model is described in detail because it produces branching fractal objects

that are similar to the patterns observed in the retinal circulation of the human retina.

Many growing, branching objects can be simulated by computer simulations in which the spatial dependence of a field (temperature, concentration, electric field, etc.) satisfies the Laplace equation with moving boundary conditions. Diffusion-limited growth is a class of these models in which the concentration of diffusing particles satisfies the Laplace equation (51).

One such model is the diffusion-limited aggregation model (DLA) formulated in 1981 by Witten & Sander (46, 57). DLA is a far from equilibrium process. In other words, DLA is a nonequilibrium process. The simulation of a DLA yields branching patterns similar to the branching patterns seen in the human retina owing to the retinal circulation of arteries and veins. The fractal dimension of diffusion-limited aggregates is usually $D = 1.71$ for a fractal embedded in a two-dimensional space (58).

THE RETINAL VASCULAR SYSTEM

The Retinal Circulation

The retina has the highest oxygen requirement per unit weight of any tissue in the body, and any alteration in circulation may result in functional impairment and tissue damage. Diseases of the retinal circulation that can lead to blindness if untreated include diabetic retinopathy, retinopathy of prematurity, and hypertensive vascular disease (59).

The retina is supplied by two major blood vessel systems (60). The inner layer (nerve fiber layer) of nerves and glial cells are supplied by the retinal circulation. The retinal circulation performs the nutritive function for the inner two-thirds of the retina. In human beings, this circulation is supplied by the central retinal artery and has one main collecting trunk, the central retinal vein. The arteries of the retinal circulation lie in the nerve fiber layer or ganglion cell layer just below the internal limiting membrane. Following bifurcation at the optic disc, the retinal artery and vein form extended branching patterns throughout the retina. The veins and arteries do not cross themselves, but a vein and an artery can overlap, forming arteriovenous crossings. There are smaller branches of these major vessels: arterioles, venules, and the smallest vessels, the capillaries. The capillaries form a vast network throughout the retina and are suspended between the arterial and venous systems. The retinal blood vessels enter and leave the retina at the optic disc (the center of each retinal image in Figures 1–4), and to the right of the optic disc is the avascular foveal region. The branching patterns of the retinal circulation in the living normal human retina are the subject of this review.

The second circulatory system of the retina is the choroidal circulation, which supplies the outer layer of the cells of the neural retina (photoreceptors) and the retinal pigment epithelium (59). The choroidal arteries and veins do not run parallel as in most vascular systems. The choroidal circulation is both a nutritive and a

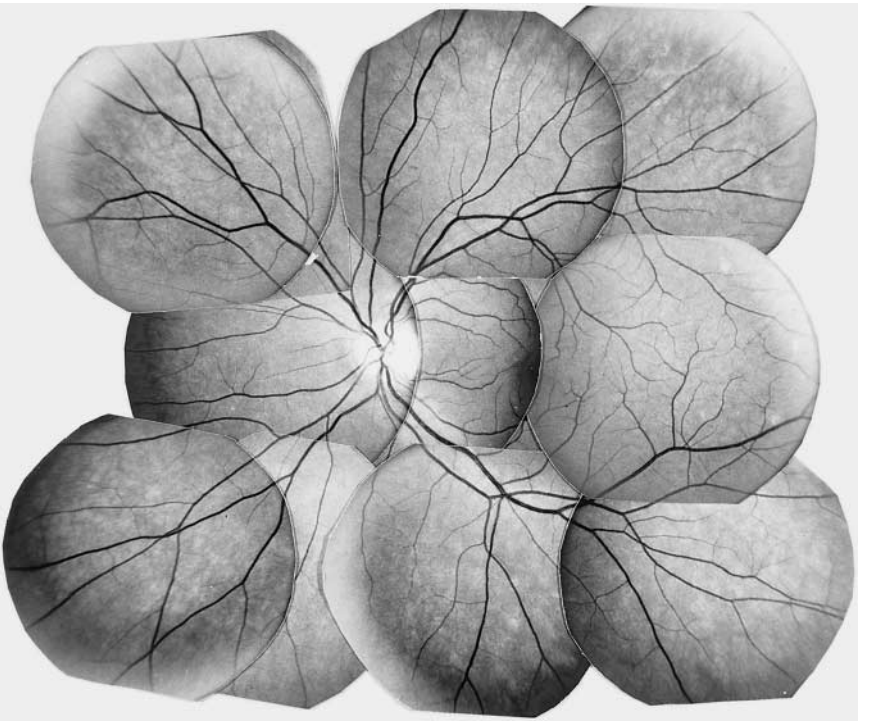

Figure 1 Photomontage of retinal fields of normal human retina taken with a red-free (green filter) retinal camera. The bright region in the center of the photomontage from which the retina blood vessels appear is the optic nerve head. The major retinal arteries and veins appear black against a lighter background of the nerve fiber layer.

cooling system for the eye. The choroidal circulation system consists of three layers of choroidal vessels. The retinal circulation is visible clinically; however, the choroidal circulation is not visible except in pigmented areas of the retina. There are image-processing techniques, e.g., indocyanine green (ICG) choroidal angiography, to characterize choroidal blood flow (61, 62).

Embryological Development of the Retinal Vascular System

In primates, the retinal vascularization proceeds via angiogenic sprouting from preexisting vessels in all regions and stages. Critical reviews of the cellular mechanisms in retinal vascular development have recently been published (63, 64).

The developing retinal vasculature may utilize novel sources of endothelial cells, such as recruitment of circulating stem cells and redeployment of mural cells from regressing vessel segments. Vascular growth occurs by two complementary mechanisms, vasculogenesis and angiogenesis. Controversy still exists over the mechanism of retinal vascular development (63). Vasculogenesis is the development of a vasculature by differentiation and organization of endothelial cell

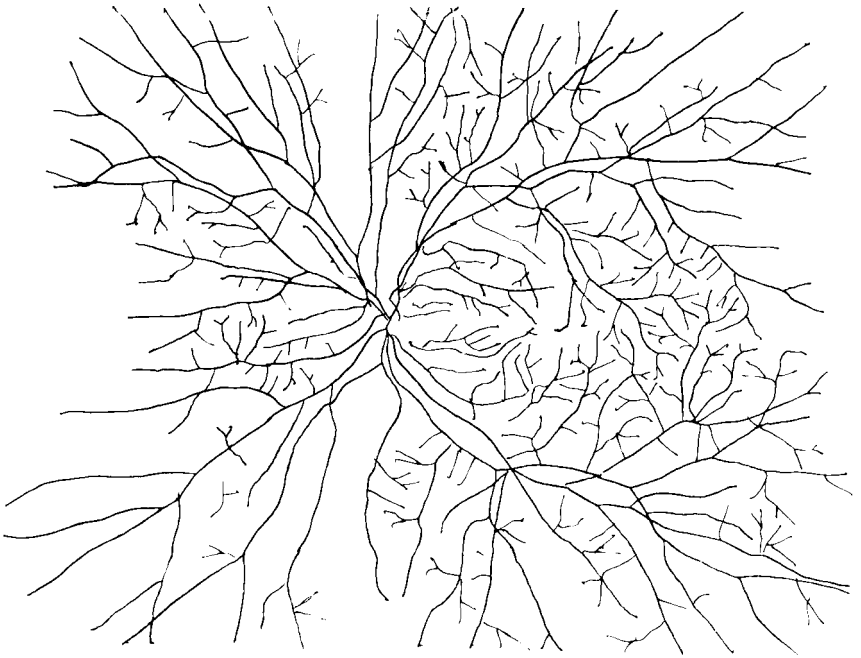

Figure 2 Tracing of the retinal vessels from the photomontage shown in Figure 1.

precursors, angioblasts. Vasculogenesis is the process by which the initial vascular tree forms from an embryonic precursor cell. Angiogenesis is the formation of a blood vessel from an existing blood vessel by the migration and proliferation of endothelial cells. Angiogenesis is the process in which new vessels arise by sprouting of budlike and fine endothelial extensions from preexisting vessels. Angiogenesis changes the vascular tree created by vasculogenesis during embryogenesis and it results in the formation of pathologic vessels in tumors and other disease states, such as proliferative diabetic retinopathy (64).

In human beings, the retina remains avascular until the fourth month of fetal development (65). Up to this point of development, the hyaloid artery, which is the only intraocular blood vessel, has no retinal branches. At the end of the four-month period, the vascular mesenchymal cells enter the nerve fiber layer. The mesenchymal spindle cells spread out toward the periphery of the retina. Vascular growth occurs outward from the disc. The development of the mature vascular system probably involves a number of variables, including hemodynamic and metabolic factors and oxygen gradients.

Endothelial cells form a single layer that lines all blood vessels. Vessels develop from the walls of existing small vessels by the outgrowth of these endothelial cells. The endothelial cells are formed by the division of existing endothelial cells. New capillaries form by sprouting from existing small vessels and develop into new vessels. This process is called angiogenesis. The growth of the capillary network may be due to angiogenic factors released by the surrounding tissues.

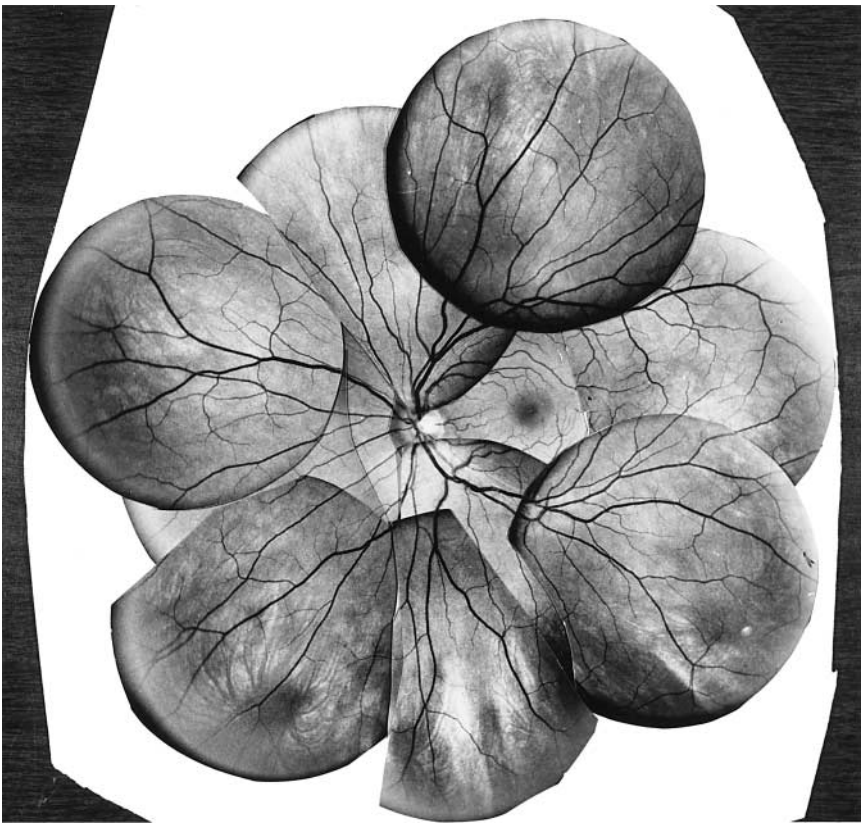

Figure 3 Photomontage of retinal fields of normal human retina taken with a red-free (green filter) retinal camera. The retinal arteries and veins appear black against a lighter background of the nerve fiber layer.

A model for the development of the inner retinal circulation has been proposed by Kretzer and colleagues (66). Their hypothesis may be summarized as follows. There is a relation between inner retinal blood vessel development and maturation of the photoreceptors. In the course of development, the maturing photoreceptors consume progressively more oxygen, decreasing the oxygen available to support the respiratory needs of the inner retina. The migrating spindle cells in the avascular inner retina sense this diminished oxygen concentration and migrate toward the area of diminished oxygen concentration. The decrease in the transretinal flux of oxygen from the choroidal vasculature is compensated by a new vascular source on the inner retina. There is a putative relationship between inner retinal vascular development and the maturation of the photoreceptors. As the photoreceptors mature, they consume more oxygen; this is indicated by the increasing number and density of the mitochondria in their inner segments.

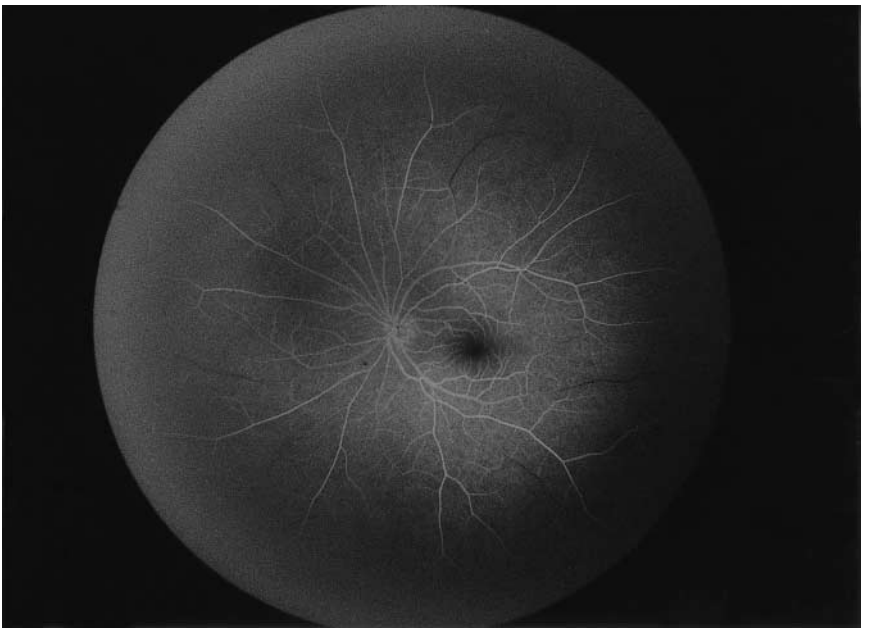

Figure 4 An example of a fluorescein angiogram of the normal human retina from another subject. The image was taken with a 140° wide-field retinal camera. The retinal vessels appear white owing to the fluorescence of the fluorescein in the vessels.

In the case of pathology, i.e., retinopathy of prematurity, the spindle cells respond with the release of angiogenic factors (66). The angiogenic factors diffuse in the plane of the retina and stimulate the growth of new retinal blood vessels and the process of neovascularization. The diffusion of angiogenic factors is the physical process responsible for the new development of retinal vessel patterns.

Local oxygen tension has a large effect on the vasculature; it compensates vascular insufficiency through the induction of angiogenesis (67). This process is thought to be mediated by the hypoxia-inducible factor (HIF) complex, which is activated in hypoxic cells and increases transcription of a broad range of genes, including angiogenic growth factors such as VEGF. An important function for the vascular architecture is to bring the circulatory system into close contact with all cells. An important research question is how the vascular architecture develops and remodels in such a manner to insure that all areas of the tissue are adequately perfused.

Fractal Analysis of the Human Retinal Circulation

The determination of the fractal dimension of the normal human retinal circulation is dependent on the quality and the type of retinal images. For a wide field of the retina to be imaged at high resolution, retinal photomontages are usually

constructed from a series of images obtained with red-free retinal cameras; that is, the use of a green filter that causes the blood vessels in the retinal circulation to appear black. Examples of these photomontages are shown in Figures 1 and 3. The arteries and veins of the retinal circulation are seen as black vessels with a much lighter nerve fiber layer in the background. Alternatively, but not recommended, is the use of fluorescein angiograms of the retina. Masters has found that fractal analysis of retinal blood vessels based on the use of fluorescein angiograms shows great variability as compared to the use of red-free images taken with a retinal camera. An example is shown in Figure 4. These images show the veins and arteries of the retinal circulation as white lines owing to the bright fluorescence of the fluorescein that was injected into the circulatory system. The vessels of the retinal circulation that appear in the fluorescein angiograms depend on the time the image was acquired following the injection of the fluorescein. In addition, there is a bright background owing to leakage of the fluorescein. Therefore, there is great variability in detecting the vessels of the retinal circulation in these images. In most of the experimental work, the blood vessels are traced as shown in Figure 2, and one of the methods to determine the fractal dimension is used. It is important to note that the fractal analysis of the normal human retinal circulation may yield different results when applied to the diseased retina; however, the great variability of the results and analysis do not form the basis of a useful diagnostic tool at this time.

The application of fractals and fractal growth processes to the branching blood vessels of the normal human retinal circulation was introduced by Masters (68, 69) who worked in collaboration with Platt and Family (68, 69). A series of papers led to an estimate of the fractal dimension for the retinal vessels of $D = 1.7$, which is in good agreement with the dimension of a diffusion-limited aggregation cluster grown in two dimensions (68, 69). The early studies had difficulty in obtaining clinical fundus images of normal subjects and were also limited by lack of standardization in the acquisition of the fundus images and the methods of analysis to determine the fractal dimension. For example, this early investigation of six subjects only contained four normals and used various types of fundus cameras to acquire the images (30°, 60°, 140°). In addition, both the mass-radius and the two-point correlation function methods were used. This diversity of subjects, image acquisition, and fractal analysis methods results in a spread of the value of the fractal dimension. However, if the study is limited to the normal, human retina, and the mass-radius analysis method, then the measured fractal dimension is 1.72, which is consistent with a diffusion-limited growth process.

Several independent research groups have demonstrated that for the normal human retina over a range of ages, the patterns of the retinal vasculature are fractal. What is extremely interesting is that the patterns resemble a particular type of fractal-DLA cluster. The normal retinal vasculature and two-dimensional DLA models have fractal dimensions of approximately 1.7. As previously discussed, these are formed by a diffusion field that is governed by the Laplace diffusion equation. This fact may have implications on the mechanism of normal retinal vasculogenesis, which is the normal formation of blood vessels.

How does this study compare with our previous studies and with the results of others? Daxer (70) calculated the fractal dimension of normal human subjects with the density-density correlation function method. He reported that 14 normals had a fractal dimension of 1.708 $\pm$ 0.073 (mean $\pm$ standard deviation). This study used red-free retinal camera photographs as the source of data (70).

Two recent studies analyzed the retinal blood vessel patterns in fluorescein angiograms made with a 60° fundus camera. Landini et al. (71) determined the fractal dimension of the retinal blood vessels of 23 normal human subjects. The fractal dimension was determined with the box-counting method. The arterial and venous trees were manually traced separately and in combination. For retinal vessels in the size range 250–3200 μm, the following fractal dimensions were calculated: arteries 1.64, veins 1.66, and arteries and veins combined 1.76. These authors did not find differences with age (14–73 years) or sex (71). This study supports the view that a nonequilibrium Laplacian process could be involved in retinal angiogenesis. They also point out that small discrepancies in the estimation of the fractal dimension by various authors are related to image acquisition techniques rather than real differences in the fractal dimension.

In another study, Mainster (72) used the mass-radius method to analyze the fractal dimension of human subjects from their fluorescein angiograms. It is important to note that these are not normal human retinas; the subjects showed early background diabetic retinopathy. The retinal arteries had a fractal dimension of 1.63, and the veins had a fractal dimension of 1.71. Mainster is in agreement with the earlier suggestion of Masters (68) that a diffusion-limited growth process, based on the Laplace equation, may be involved in the development of the retinal blood vessel patterns (72).

One study of the fractal dimension of the normal human retinal circulation met all the criteria of standardized image acquisition, image tracing, and analysis (73, 74). The mean value and standard deviation of the fractal dimension (box-counting dimension) is 1.70 $\pm$ 0.02 (N = 10). All of the red-free images were obtained with a Zeiss fundus camera with a 30° field of view. A single ophthalmic photographer photographed all of the subjects. The subjects were previously examined by an ophthalmologist and were devoid of retinal pathology. The use of standard methods for both the data acquisition and the data analysis resulted in less variance in the data than was reported in our previous studies. In the limited sample, there were no differences between left and right eyes, nor with age in the range of 25–38 years (Table 1).

The blood vessel patterns of the retinal circulation of the normal human eye are self-similar structures with a fractal dimension (box counting dimension) of approximately 1.7. (74). This is the same fractal dimension that is found for a diffusion-limited growth process. The pattern is therefore consistent with the hypothesis that the development of human retinal blood vessels involves a diffusion process (75).

Two recent papers develop DLA from shear stress as a simple model of vasculogenesis (76). A model is proposed in which the formation of the vascular network

TABLE 1 Fractal dimension (Bos-counting method) of the normal human retinal blood vessel patterns (74)

Name[a]	Age	Eye[b]	Fractal dimension
AHS	38	OS	1.70
AHS	38	OD	1.69
BHS	25	OS	1.68
CHS	28	OD	1.71
DHS	32	OD	1.72
DHS	32	OS	1.71
EHS	34	OS	1.71
EHS	34	OD	1.72
FHS	25	OD	1.68
FHS	25	OS	1.68

[a]Initials of each subject.

[b]OD, right eye; OS, left eye.

proceeds via a progressive penetration of the vessel ramification into a capillary mesh. The driving force is of hydrodynamic origin and results in a Laplacian growth mechanism. In their model, the growth of both arteries and veins follows the directions of high shear stress provoked by the blood flow on the endothelium wall of a preexisting capillary mesh. Their growth is driven by a field that satisfies the Laplace equation. This imposes a growth velocity on the tree surface that is proportional to the gradient of the field. The higher the flux, the higher the growth speed. Vasculogenesis occurs early in the growth process. There are two processes of vascular growth. The first is the transformation of cells into fibroblasts and endothelial cells. This results in the random formation of capillaries. The second is the proliferation and migration of endothelial cells found in the first vascular structure, which results in sprouting into previously avascular organs. The remodeling of the capillary network results in the formation of small vessels, which then enlarge in a process of maturation called pruning. The modeling of three-dimensional microvasculature by interlaced DLA includes a model of three-dimensional vascular formation, which is able to explain how the capillary system matures into two three-dimensional arborescent vasculatures, which interdigitate in the distal parts (77).

LIMITATIONS OF FRACTAL ANALYSIS OF BRANCHING BIOLOGICAL STRUCTURES

It is important to understand the experimental and the theoretical limitations of the application of fractal analysis to the branching blood vessels of the normal human retinal circulation.

To achieve high precision and accuracy in the experimental determination of the fractal dimension of the branching patterns of the human retinal circulation, it is important to adhere to the following procedures. A single fundus photographer should acquire the retinal images of the normal subjects using the same retinal camera. The photomontages of the red-free fundus images should be made by the same person. The tracings of the branching vessels in the retinal circulation should be made by the same person. Comparison of the fractal dimension using the density-density correlation method does not always agree with the fractal dimension obtained from the same subjects using the box-counting or mass radius method owing to the subjective fit of the curve to a straight line, which introduces error. It was also observed that comparison of branching vessel patterns from red-free fundus photographs and their montages to obtain a wide field do not always agree with similar studies based on a fluorescein angiogram.

Some of these sources of error and discrepancies in the estimation of the fractal dimension have been previously discussed (78). Many of the variations in the experimental determination of the fractal dimension discussed in this paper can be attributed to the comparison of red-free retinal photographs with fluorescein angiograms in which the time of the image capture affects the visibility of the arteries and the veins in the retinal circulation, comparison of normal retinal with subjects showing disease states (e.g., 72), and comparison of computerized box-counting techniques with the more variable and subjective density-density correlation methods.

An alternative explanation for the different values of the fractal dimensions evaluated by different groups (79) is the crossover effect of several different fractal dimensions. However, the major differences discussed in the preceding paragraph were not addressed, i.e., use of subjects with retinal disease and use of subjective selection of a particular image from the set of angiograms.

The fractal dimension does not uniquely characterize the shape or form of the fractal object. It is a measure of how the fractal object fills up space. Nevertheless, there is some correspondence between the observed complexity or roughness of a pattern and its fractal dimension. As the complexity of how the object fills up space increases, the fractal dimension increases. In a plane, if the object is completely space filling, the fractal dimension is two. It is important to realize that there is not a unique relation between the shape of a pattern and its fractal dimension. Various patterns that fill space in the same way and show similar scaling relations have the same fractal dimension. Nevertheless, the single number may have important significance in characterizing the process that led to the formation of the pattern as a feature descriptor of the pattern.

What are the possible limitations of the preceding methodology? The mass-radius method assumes that the mass (the size of the object) is to be determined. The tracings convert a pattern comprised of vessels with a length and a width to a pattern comprised of lines. It is equivalent to having a vessel with an average width that does not vary with distance from the optic nerve head.

The geometry of the eye could also affect the experimental determination of the fractal dimension. A projection from a two-dimensional curved surface to a

two-dimensional flat surface was used to produce a photograph of the retinal vessels. This projection involved the introduction of a fixed-length scale—the radius of curvature of the eye. Asymptotically, the measurement of the fractal dimension should not be sensitive to such an effect. In addition, the projection of a fractal embedded in three dimensions to a plane of two dimensions does not change D so long as the condition of $D < d$ holds. In the case of retinal blood vessels, D is approximately 1.7 and the Euclidean dimension is 2 for a plane. Therefore, the condition of $D < d$ is valid (56). Finally, it must be stated that the analysis was made over a limited range of length scales (approximately two decades) and therefore the conclusions are valid only in this regime.

Several studies attempt to use differences in the fractal dimension as a discriminant factor to detect and diagnose disease. The global analysis of the retinal circulation may miss the very early changes in the microvascular systems of the retinal circulation and, therefore, not be sensitive to the early manifestation of disease. Many disease processes show their first manifestations in the microvascular systems of the retina, and the studies covered in this review do not investigate the microvascular systems (80). Major alterations of the vessels in the retinal circulation would manifest themselves as alterations in the fractal dimension.

In addition to the fractal dimension, the property of lacunarity may be an additional useful discriminant in the study of branching blood vessels. Lacunarity is a measure of the size of gaps or holes within a structure and may complement the fractal dimension in the characterization of texture (81, 82).

Finally, however useful fractal analysis is to the study of the vascular system, it still suffers from the fundamental problem that it is not based on fundamental physical laws that can be expressed in mathematical form. Each branch of physics, from mechanics to thermodynamics, to electric and magnetic field theory, to quantum mechanics, to fluid flow, has fundamental physics laws that govern the phenomena. There is no fundamental equation that governs fractal geometry.

OPTIMAL ORGANIZATION OF VASCULAR TREES AND THE HUMAN BRONCHIAL TREE

If we may assume that the design of branching biological trees, e.g., the human bronchial tree and the human retinal circulation, follows optimization principles, then a reasonable question to ask is what should be optimized? There are several general references that attempt to answer this question (19, 83–85).

There are many publications on the optimal organization of branching trees. Two early papers that developed the principles of optimal organization of branching trees were the work of Murray (86, 87). In 1926, Murray developed the principle of minimum work. He simultaneously minimized the energy-equivalent cost of blood flow and blood volume and concluded that the optimal economy of circulation can be realized if the flow is everywhere proportional to the third power of the vessel's

diameter. This relationship is valid for the general flow in the entire vasculature; the flows in the individual vessels may differ owing to local conditions. A second paper by Murray applied the physiological principle of minimum work to the angle of branching arteries. The Murray Principle is based on Poisseuille's law for the flow of liquids in tubes. It was shown that the diameter, d, of a blood vessel is optimum when it is proportional to the cube root of the flow, q, in the vessel. Thus, the flow of blood past any section of artery shall be related to the cube of the radius of the vessel at that point.

The application of the Murray Principle to the normal human retinal circulation has been validated (88, 89). An advantage of study of the retinal vascular system is that in the retina, a large number of arterial bifurcations can be easily studied in vivo.

Horsfield (20) made a similar application of an optimization principle to the morphology of the bronchial tree in man. These authors used casts of the human bronchial tree and applied the principle of minimal work. This required that the airways of the human bronchial tree should have a maximum radius for minimal resistance to air flow. There is also a requirement that the airways should have a minimal volume for economy of space. The authors concluded that the morphology of the bronchial tree is appropriate to the function of airflow in the upper region of the tree and to molecular diffusion in the distal region, while maintaining a minimal volume compatible with these functions.

Another more recent application of the Murray Principle to optimal radii in microvascular networks makes the prediction that the flow is proportional to the cube of the vessel radius, and that at vessel junctions, the cube of the radius of the parent vessel equals the sum of the cubes of the daughter radii (90). This follows from the conservation of flow at vessel junctions. The authors studied the traverse arteriolar trees of the cat sartorius muscle and concluded that for entire trees with many junctions, the departure from the Murray Principle was small in energy terms.

Mayrovitz & Roy (91) tested the functional relationship between microvascular blood flow and arteriolar internal diameter. They studied paired blood velocity and arteriolar diameter in the cremaster muscle microvasculature of rats and concluded that for this vascular system, the flow is proportional to the cube of the diameter of the vessels (91).

In conclusion, design of the branching patterns of the human retinal circulation and the relation between vessel size and blood flow have been validated as first stated in the Murray Principle of 1926.

CONCLUSIONS AND FUTURE DIRECTIONS

The biological mechanism for the formation of retinal vessel patterns in the developing human eye is unknown even though it is a question of importance. The current hypothesis is based on the existence of a variable oxygen gradient across

the developing photoreceptors that stimulates the release of angiogenic factors, which diffuse in the plane of the retina and result in the growth of retinal vessels. This implies that the rate-limiting step in the formation of the vessel pattern is a diffusion process.

The branching patterns of the blood vessels in the normal human retinal circulation have a self-similar structure with a fractal dimension of approximately 1.7. This is the same fractal dimension found for a diffusion-limited growth process, and this is consistent with the hypothesis that the development of human retinal vessels involves a diffusion process. Furthermore, the experimental data supports the Murray Principle, i.e., the diameter of an artery is approximately proportional to the cube root of the flow that the artery is designed to convey (92).

Given that the normal human retinal circulation is a self-similar, fractal pattern, and that the Murray optimization principle is valid for the blood vessels in the normal human retinal circulation, it is exciting to pose the following question: What is the link, if any, between the observed fractal pattern and the theoretical formulation of the Murray principle? It is of interest to derive the fractal properties of the normal human retinal circulation from the Murray Principle.

The diagnostic potential of fractal analysis of the branching patterns of the blood vessels in the retinal circulation has not been demonstrated with high sensitivity and high specificity. This may be due to the fact that many retinal microvascular abnormalities occur early in the disease process, they are located in the capillaries, and result in alterations of permeability.

There is also the question of why fractals.

It has been suggested that fractal models have an appeal in that they are simple to encode genetically because the same branching mechanism is used repeatedly (93).

Fractal analysis of blood vessels may also find applications in the design and development of perfusion systems in artificial organs, e.g., kidney and liver, in which optimal exchange of metabolic components is desirable.

ACKNOWLEDGMENTS

This work was supported by a grant from NIH, National Eye Institute, EY-06958. I thank Dr. Stephen Sinclair for providing the red-free montages of the human retinas.

The *Annual Review of Biomedical Engineering* is online at http://bioeng.annualreviews.org

LITERATURE CITED

1. Wong D. 1991. The fundus camera. In *Duane's Clinical Ophthalmology*, eds. W Tasman, EA Jaeger, 61:1–14. Philadelphia, PA: J.B. Lippincott
2. Rashevsky N. 1960. *Mathematical Biophysics. Physico-Mathematical Foundations of Biology*. New York: Dover Publ. 3rd ed.

3. West BJ. 1990. *Fractal Physiology and Chaos in Medicine*. Singapore: World Sci.
4. Schroeder M. 1991. *Fractals, Chaos, Power Laws: Minutes from an Infinite Paradise*. San Francisco: W.H. Freeman. 429 pp.
5. Bassingthwaighte JB, Liebovitch LS, West BJ. 1994. *Fractal Physiology*. New York: Oxford Univ. Press
6. Iannaccone PM, Khokha M, eds. 1996. *Fractal Geometry in Biological Systems, An Analytical Approach*. Boca Raton, FL: CRC Press. 360 pp.
7. Stanley HE, Amaral LAN, Buldyrev SV, Goldberger AL, Havlin S, et al. 1996. Scaling and universality in living systems. *Fractals* 4:427–51
8. Smith TG Jr, Marks WB, Lange GD, Sheriff WH Jr, Neale EA. 1989. A fractal analysis of cell images. *J. Neurosci. Methods* 27:173–80
9. Caserta F, Stanley HE, Eldred WD, Daccord G, Hausman RE, Nittmann J. 1990. Physical mechanisms underlying neurite outgrowth: a quantitative analysis of neuronal shape. *Phys. Rev. Lett.* 64:95–98
10. Porter R, Ghosh S, Lange GD, Smith TG Jr. 1991. A fractal analysis of pyramidal neurons in mammalian motor cortex. *Neurosci. Lett.* 130:112–16
11. Reichenbach A, Siegel A, Senitz D, Smith TG Jr. 1992. A comparative fractal analysis of various mammalian astroglial cell types. *Neuroimage* 1:69–77
12. Smith TG Jr, Behar TN, Lange GD, Marks WB, Sheriff WH Jr. 1991. A fractal analysis of cultured rat optic nerve glial growth and differentiation. *Neuroscience* 41:159–66
13. Goldberger AL, Peng C-K, Hausdorff J, Mietus J, Havlin S, Stanley HE. 1996. Fractals and the heart. See Ref. 6, pp. 249–66
14. Einstein AJ, Wu H-S, Gil G. 1998. Self-affinity and lacunarity of chromatin texture in benign and malignant breast epithelial cell nuclei. *Phys. Rev. Lett.* 80:397–400
15. Peiss J, Verlande M, Ameling W, Gunther RW. 1996. Classification of lung tumors on chest radiographs by fractal texture analysis. *Invest. Radiol.* 31:625–29
16. Floyd CE Jr, Patz EF, Lo JY, Vittitoe NF, Stambaugh LW. 1996. Diffuse nodular lung disease on chest radiographs: a pilot study of characterization by fractal dimension. *Am. J. Radiol.* 167:1185–87
17. West BJ, Bhargava V, Goldberger AL. 1986. Beyond the principle of similitude: renormalization in the bronchial tree. *J Appl. Physiol.* 60:189–97
18. Uppaluri R, Hoffman EA, Sonka M, Hartley PG, Hunninghake GW, McLennan G. 1999. Computer recognition of regional lung disease patterns. *Am. J. Respir. Crit. Care Med.* 160:648–54
19. Weibel ER. 1963. *Morphometry of the Human Lung*. Berlin: Springer-Verlag
20. Horsfield K, Cumming G. 1967. Angles of branching and diameters of branches in the human bronchial tree. *Bull. Math. Biophys.* 29:245–59
21. Weibel ER. 1987. Scaling of structural and functional variables in the respiratory system. *Annu. Rev. Physiol.* 49:147–59
22. Horsfield K, Cumming G. 1968. Morphology of the bronchial tree in man. *J. Appl. Physiol.* 24:373–83
23. Horsfield K, Dart G, Olson DE, Filley GF, Cumming G. 1971. Models of the human bronchial tree. *J. Appl. Physiol.* 31:207–17
24. Horsfield K. 1978. Morphometry of the small pulmonary arteries in man. *Circ. Res.* 42:593–97
25. Sernetz M, Justen M, Jestczemski F. 1995. Dispersive fractal characterization of kidney arteries by three-dimensional mass-radius-analysis. *Fractals* 3:879–91
26. Masters BR, Family F, Platt DE. 1989. Fractal analysis of human retinal vessels. *Biophys. J.* 55:575a (Suppl.)
27. Masters BR. 1989. Fractal analysis of human retinal vessels. *SPIE Proc.* 1357:250–56
28. Masters BR. 1989. Fractal analysis of human retina blood vessel patterns: developmental aspects. *Int. Symp. Ocular Circ. Neovascularization, 2nd, Wilmer*

Inst., Johns Hopkins Med. Inst., p. 45. Baltimore, MD
29. Tsonis AA, Tsonis PA. 1987. Fractals: a new look at biological shape and patterning. *Perspect. Biol. Med.* 30:355–60
30. Wornell GW. 1998. Fractal signals. In *The Digital Signal Processing Handbook*, ed. VK Madisetti, DB Smith, pp. 73-1–13. Boca Raton, FL: CRC Press
31. Goldberger AL, Bhargava V, West BJ, Mandell AJ. 1985. On a mechanism of cardiac electrical stability: the fractal hypothesis. *Biophys. J.* 48:525–28
32. Liebovitch LS. 1996. Ion channel kinetics. See Ref. 6, pp. 31–56
33. Folkman J. 1976. The vascularization of tumors. *Sci. Am.* 234:58–73
34. Folkman J, Haudenschild C. 1980. Angiogenesis in vitro. *Nature* 288:551–56
35. Yancopoulos GD, Klagsbrun M, Folkman J. 1998. Vasculogenesis, angiogenesis, and growth factors: ephrins enter the fray at the border. *Cell* 93:661–64
36. Masters BR. 1990. Fractal analysis of human retinal blood vessel patterns: developmental and diagnostic aspects. In *Noninvasive Diagnostic Techniques in Ophthalmology*, ed. BR Masters, pp. 515–27. New York: Springer Verlag
37. Landini G, Misson GP. 1993. Simulation of corneal neovascularization by inverted diffusion limited aggregation. *Invest. Ophthalmol. Vis. Sci.* 34:1872–76
38. Thompson DW. 1942. *On Growth and Form*. Cambridge: Cambridge Univ. Press
39. Stanley HE, Ostrowsky N, eds. 1986. *On Growth and Form*. Dordrecht: Martinus Nijhoff
40. West GB, Brown JH, Enquist BJ. 1997. A general model for the origin of allometric scaling laws in biology. *Science* 276:122–26
41. Cook TA. 1979. *The Curves of Life*. New York: Dover Publ.
42. Ball P. 1999. *The Self-Made Tapestry: Pattern Formation in Nature*. New York: Oxford Univ. Press
43. Livio M. 2002. *The Golden Ratio: The Story of Phi, The World's Most Astonishing Number.* New York: Random House
44. Mandelbrot BB. 1967. How long is the coast of Britain? Statistical self-similarity and fractional dimension. *Science* 156:636–38
45. Mandelbrot BB. 1982. *The Fractal Geometry of Nature*. San Francisco: WH Freeman. 460 pp.
46. Sander LM. 1987. Fractal Growth. *Sci. Am.* 256:94–100
47. Ben-Jacob E, Garik P. 1990. The formation of patterns in non-equilibrium growth. *Nature* 343:523–30
48. Peitgen H-O, Jürgens H, Saupe D. 1992. *Chaos and Fractals. New Frontiers of Science*. Berlin: Springer-Verlag. 984 pp.
49. Feder J. 1988. *Fractals*. New York: Plenum
50. Falconer K. 1997. *Techniques of Fractal Geometry*. New York: Wiley
51. Pietronero L, Erzan A, Evertsz C. 1988. Theory of Laplacian fractals: diffusion limited aggregation and dielectric breakdown model. *Physica A* 151:207–45
52. Vicsek T. 1992. *Fractal Growth Phenomena*. Singapore: World Sci. 488 pp. 2nd ed.
53. Landini G. 1996. Applications of fractal geometry in pathology. See Ref. 6, pp. 205–46
54. Bittner HR, Wlczek P, Sernetz M. 1989. Characterization of fractal biological objects by image analysis. *Acta Stereol.* 8:31–40
55. Bunde A, Havlin S, eds. 1991. *Fractals and Disordered Systems*. New York: Springer-Verlag
56. Weitz DA, Oliveria M. 1984. Fractal structures formed by kinetic aggregation of aqueous gold colloids. *Phys. Rev. Lett.* 52: 1433–36
57. Witten TA, Sander LM. 1981. Diffusion-limited aggregation, a kinetic phenomena. *Phys. Rev. Lett.* 47:1400–3
58. Meakin P. 1986. A new model for biological pattern formation. *J. Theor. Biol.* 118: 101–13
59. Ryan SJ. 1989. *Retina*. St. Louis: Mosby. Vols. 1, 2, 3

60. Hogan MJ, Alvarado JA, Weddel JE. 1971. *Histology of the Human Eye*. Philadelphia, PA: Saunders
61. Klein GJ, Baumgartner RH, Flower RW. 1990. An image processing approach to characterizing choroidal blood flow. *Invest. Ophthalmol.* 31:23–31
62. Lambrou GN. 1993. *Choroidal Plerometry: A Method for Evaluating the Choroidal Blood Supply in Clinical Practice*. The Hague: Kugler Publ.
63. Lutty GA, McLeod DS. 2003. Retinal vascular development and oxygen-induced retinopathy: a role for adenosine. *Prog. Retin. Eye Res.* 22:95–111
64. Gariano RF. 2002. Cellular mechanisms in retinal vascular development. *Prog. Retin. Eye Res.* 22:295–306
65. Ozanics V, Jakobiec FA. 1982. Prenatal development of the eye and its adnexa. In *Ocular Anatomy, Embryology and Teratology*, ed. FA Jakobiec, pp. 11–96. Philadelphia, PA: Harper Row
66. Kretzer FL, Hittner HM. 1988. Retinopathy of prematurity: clinical implications of retinal development. *Arch. Dis. Child.* 63:1151–67
67. Maxwell PH, Ratcliffe PJ. 2002. Oxygen sensors and angiogenesis. *Cell Develop. Biol.* 13:29–37
68. Masters BR, Platt DF. 1989. Development of human retinal vessels: a fractal analysis. *Invest. Ophthalmol. Vis. Sci.* 30:391 (Suppl.)
69. Family F, Masters BR, Platt DE. 1989. Fractal pattern formation in human retinal vessels. *Physica D* 38:98–103
70. Daxer A. 1993. Fractal analysis of new vessels in diabetic retinopathy. *Invest. Ophthalmol. Vis. Sci.* 34(Suppl.):718
71. Landini G, Misson GP, Murray P. 1993. Fractal analysis of the normal human retinal fluorescein angiogram. *Curr. Eye Res.* 12:23–27
72. Mainster MA. 1990. The fractal properties of retinal vessels: embryological and clinical implications. *Eye* 4:235–41
73. Masters BR, Sernetz M, Wlczek P. 1992. Image analysis of human retinal blood vessels and their characterization as fractals. *Acta Stereol.* 11(Suppl. 1):355–60
74. Masters BR. 1994. Fractal analysis of normal human retinal blood vessels. *Fractals* 2:103–10
75. Masters BR. 1991. Fractal patterns in the human retina and their physiological correlates. *Proc. SPIE* 1380:218–26
76. Fleury V, Schwartz L. 1999. Diffusion limited aggregation from shear stress as a simple model of vasculogenesis. *Fractals* 7:33–39
77. Fleury V, Schwartz L. 2000. Modelisation of 3-D microvasculature by interlaced diffusion limited aggregation. *Fractals* 8:255–59
78. Kyriacos S, Nekka F, Cartilier L, Vico P. 1997. Insights into the formation process of the retinal vasculature. *Fractals* 5:615–24
79. Sun T, Meakin P, Jossang T. 1995. Minimum energy dissipation and fractal structures of vascular systems. *Fractals* 3:123–53
80. Wong TY, Klein R, Klein BEK, Tielsch JM, Hubbard L, Nieto FJ. 2001. Retinal microvascular abnormalities and their relationship with hypertension, cardiovascular disease, and mortality. *Surv. Ophthalmol.* 46:59–80
81. Obert M. 1993. Numerical estimates of the fractal dimension D and the lacunarity L by the mass radius relation. *Fractals* 1:711–21
82. Landini G, Murray P, Misson GP. 1995. Local connected fractal dimensions and lacunarity analysis of 60° fluorescein angiograms. *Invest. Ophthalmol. Vis. Sci.* 36: 2749–55
83. Meinhardt H. 1982. *Models of Biological Pattern Formation*. London: Academic. 225 pp.
84. MacDonald N. 1983. *Trees and Networks in Biological Models*. New York: Wiley. 215 pp.
85. LaBarbera M. 1990. Principles of design of fluid transport systems in zoology. *Science* 249:992–1000

86. Murray CD. 1926. The physiological principle of minimum work. I. The vascular system and the cost of blood volume. *Proc. Natl. Acad. Sci.* USA. 12: 207–14
87. Murray CD. 1926. The physiological principle of minimum work applied to the angle of branching arteries. *J. Gen. Physiol.* 9: 835–41
88. Zamir M, Medeiros JS, Cunningham TK. 1979. Arterial bifurcations in the human retina. *J. Gen. Physiol.* 74:537–48
89. Zamir M. 2001. Fractal dimensions and multifractility in vascular branching. *J. Theor. Biol.* 212:183–90
90. Sherman TF, Popel AS, Koller A, Johnson PC. 1989. The cost of departure from optimal radii in microvascular networks. *J. Theor. Biol.* 136:245–65
91. Mayrovitz HN, Roy J. 1983. Microvascular blood flow: evidence indicating a cubic dependence on arteriolar diameter. *Am. J. Physiol. Heart Circ. Physiol.* 245(14):H1031–38
92. Zamir M, Medeiros JA, Cunningham TK. 1979. Arterial bifurcations in the human retina. *J. Gen. Physiol.* 74:537–48
93. Metzger RJ, Krasnow MA 1999. Genetic control of branching morphogenesis. *Science* 284:1635–39

Annual Review of Biomedical Engineering
Volume 6, 2004

CONTENTS